Engineered Science

RESEARCH PAPER

View Article Online

Microwave Popped Co(II)-Graphene Oxide Hybrid: Bifunctional Catalyst for Hydrogen Evolution Reaction and Hydrogen Storage

Lin Wei,[1] Karen Lozano [2] and Yuanbing Mao *[1,3]

In an effort to develop a multifunctional catalyst for hydrogen generation and adsorption applications, a facile and cost-effective microwave popping method was used to synthesize popped graphene oxide (PGO) and Co-PGO hybrid. Both samples have been explored and compared as hydrogen storage materials and as electrocatalysts for hydrogen evolution reaction (HER) for the first time. The loading of Co(II) species on the surface of the PGO enhanced the hydrogen storage capability of PGO from 0.04wt% to 0.08wt% as measured at 293K and 800 mmHg. Co-PGO is also acting as a better electrocatalyst for HER compared to the PGO counterpart.

Keywords: Cobalt; Popping Graphene Oxide; Hydrogen Storage; Hydrogen Evolution Reaction

Received 29th April 2018, Accepted 3rd June 2018

DOI: 10.30919/es8d723

1. Introduction

Development of low cost functional materials has attracted intensive research interest in recent years for eco-friendly energy conversion and energy conservation processes.[1] Among these processes, catalysts play vital roles in applications like water splitting and hydrogen spillover.[2–4] While the hydrogen spillover can facilitate hydrogenation reactions, it is also useful for hydrogen storage.[5–8] The spillover hydrogen atoms are stably stored on high-surface-area materials along with physisorbed H_2 molecules at ambient temperature. Therefore, the total hydrogen storage amount becomes larger when compared to only physisorption.[9–11] While hydrogen spillover is a well-known phenomenon in supported metal catalysts, such as Pt, Pd, Ni, and Ru, the replacement of these noble metals by cheap metal-free materials and transition metals has become a hot topic in current catalyst research.[12,13] To enhance the efficiency of hydrogen storage materials based on the spillover mechanism, the making of smaller metal nanoparticles and increasing of the adsorbent's surface area are venues to pursue.[4,12] For hydrogen storage by the spillover mechanism, transition metal/carbon hybrids have been studied broadly but only very few reports on Co/carbon hybrids have been reported.[4,12]

There is an urgent and critical need to design and develop active and efficient electrocatalysts from earth-abundant materials for water electrolysis to confront the sustainable energy-powered economy.[14–17] Among a wide variety of materials explored by scientists, cobalt and its derivatives encapsulated in carbon layers have been used for water electrolysis reactions such as hydrogen evolution reaction (HER),[18] oxygen reduction reaction (ORR),[19] and oxygen evolution reaction (OER).[20] For example, Wang et al. reported the development of Co-C-N complex for HER.[21] Jin et al. studied Co-CoO/N-doped carbon, which demonstrated excellent performance for HER and OER.[20] As a bifunctional material, the Co-CoO/N-doped carbon had shown promising potential as a water splitting catalyst.

Carbon materials such as graphene, carbon nanotubes, and activated carbon are promising candidates to meet the demand of the hydrogen economy because of their high surface areas and porous structures.[4] In recent years, graphene and its derivatives have become the golden carbon materials, these, have attracted considerable attention from government, academia and industry. In terms of preparation methods, the modified Hummer method is currently the most commonly used technique to synthesize graphene oxide (GO).[22] As-synthesized GO samples are rock-like solid with low surface area after drying due to restacking. Therefore, they are usually disperse into solutions to exfoliate GO layers. Besides exfoliation in water and other solvents,[23,24] dry exfoliation methods are also been studied. Gao *et al*. found that GO could be "popped" at 180°C and the surface area of the generated popping graphene oxide (PGO) increased greatly from 8.2 m^2/g to 400.5 m^2/g.[25] Zhu *et al.* observed significant expansion of GO accompanied by "violent fuming", exfoliation and reduction of GO could be completed in one min with 700 W of microwave irradiation.[26] The popping property

[1] *Department of Chemistry, University of Texas Rio Grande Valley, 1201 West University Drive, Edinburg, Texas 78539, USA. E-mail: yuanbing.mao@utrgv.edu*
[2] *Department of Mechanical Engineering, University of Texas Rio Grande Valley, 1201 West University Drive, Edinburg, TX 78539, USA*
[3] *School of Earth, Environmental, and Marine Sciences, University of Texas Rio Grande Valley, 1201 West University Drive, Edinburg, Texas 78539, USA. E-mail: yuanbing.mao@utrgv.edu*

of GO could enable us to synthesize reduced graphene samples without introducing any reducing agent and provide a new way to prepare metal/carbon hybrids.

However, PGO has not been loaded with cobalt species for hydrogen storage and generation applications. Herein, we aim to design a novel and cost effective material with both hydrogen adsorption and hydrogen generation activities. The popping method was used to synthesize the novel transition metal-graphene hybrid, more specifically, Co-PGO, for hydrogen storage and evolution reaction.

2. Experimental section

2.1. Materials

Nitric acid (ACS reagent, 70%), Nafion solution (20%), and hydrogen peroxide (30-32%) were purchased from Sigma-Aldrich. Graphite powder (APS, 7-11 micron, 99%) and potassium permanganate (98%) were obtained from Alfa Aesar. Sulfuric acid was purchased from Acros. Cobalt chloride hexahydrate and hydrochloric acid were obtained from Fisher Scientific. All chemicals were used as received without further purification.

2.2. Synthesis of GO

GO was synthesized by the modified Hummer method. First 1-gram graphite was dispersed into a mix solvent of 50 mL H_2SO_4 and 50 mL HNO_3 within an ice water bath. To prevent introduction of Na^+ ions, HNO_3 was used instead of $NaNO_3$. After stirring for 20 min, 5 g of $KMnO_4$ were added into the mixture and kept for reaction for 2 hours. Then the ice water bath was removed, and 100 mL of water were added into the solution to increase its temperature to room temperature and kept for 15 min. To stop the high temperature reaction, 100 mL of water were added. Finally 10 mL of a H_2O_2 solution were added into the system. After the reaction was completed, a 10% HCl solution was used for the first wash followed by copious water washes until a neutral pH was reached. The obtained GO sample was finally dried in a vacuum oven at 65°C.

2.3. Synthesis of PGO

The as-synthesized GO was placed in a beaker and microwaved for 2 minutes in a domestic (700 W) oven.

2.4. Synthesis of Co-PGO

0.0404 g $CoCl_2{\cdot}6H_2O$ and 0.1 g of the as-synthesized GO were added into 2 mL of water. The mixture was sonicated for 15 min and then kept overnight in a vacuum oven at 60°C. After drying, it was transferred into a beaker and heated in a domestic microwave oven (700 W) for 2 minutes.

2.5. Characterizations

The morphology of the PGO and Co-PGO samples was investigated by a field-emission scanning electron microscopy (FESEM, Sigma VP Carl Zeiss, Germany). Energy-dispersive spectroscopy (EDS) was used to analyze the elements within these composites. Powder X-ray diffraction (XRD) patterns were taken with a Rigaku Miniflex diffractometer. Fourier Transform Infrared (FT-IR) spectra were collected with a Thermo Nicolet NEXUS 670. Raman spectra were taken by a SENTERRA Dispersive Raman Microscope. X-ray photoelectron spectroscopy (XPS) was performed in a Thermo Scientific Kα spectrometer with monochromatic Al kα radiation (1486.6 eV). The peak areas and atomic percentage were quantified by its accompanying Thermo Avantage software. Porosimetry analysis (BET surface area, BJH pore volume/pore area) was performed on a Micromeritics ASAP 2020 Surface Area and Porosity Analyzer. A reference material (silica-alumina) provided by Micromeritics Company was tested to assure the accuracy of the equipment. Nitrogen adsorption analyses were performed at 77 K after a preparatory degassing at 300 °C, 2 μm Hg pressure for > 8 hours. Hydrogen adsorption analyses were performed at room temperature (293 K) after the same degassing procedure.

2.6. Electrochemistry test

HER activities were measured on an AUTOLAB PGSTAT302N (Metrohm) Potentiostate/Galvanostat Instrument, which is equipped with a three-electrode system in 1 M H_2SO_4 solution. A glassy carbon electrode (3 mm diameter) coated with the ink from the as-prepared PGO or Co-PGO catalyst was used as the working electrode with scanning rate of 20 mV/s. An Ag/AgCl electrode was used as reference electrode, and a Pt wire was used as the counter electrode. The ink was prepared as follow: a mixture of 4 mg catalyst sample (PGO or Co-PGO), 20 μL 20wt% Nafion solution, and 200 μL ethanol/water (4:1) was sonicated for 1.5 hr. The electrode ink mixture was then drop casted onto the glassy carbon electrode and air dried.

3. Results and discussion

Due to microwave energy, water vapor could be generated between GO layers from –OH groups, and the amount of –OH groups between graphene oxide layers oscillate.[26] This phenomenon was studied by Gao *et al*. for the thermal popping of graphene oxide.[25] They used IR to confirm that the liquid product after popping of GO was water and the loss of -OH groups from GO was confirmed. Superheated vapor pressure between GO layers results in exfoliation and reduction of GO, a popcorn-like behavior. Figure 1 shows the curly surface of PGO and Co-PGO, which is due to the generated pressure from the superheated vapor. However, Co NPs are not observed on the PGO sheets though EDS data confirmed the existence of Co and Cl, which could have been originated from the used precursor $CoCl_2$.

Figure 2 shows the XRD patterns of PGO and Co-PGO. The XRD peak at 25° belongs to the disordered carbon, which represents the disordered popping GO layers. Co-PGO did not show any peak attributed to Co metal, or it has a relatively low intensity, hard to observe. However, from EDX analysis, Co exists in the Co-PGO sample. We believe that cobalt in Co-PGO is ionic cobalt or atomic cobalt. Since it is amorphous, it does not appear in the XRD pattern. This assumption is in agreement with the XPS results of the Co-PGO sample shown in Figure 4.

Figure 3 shows the Raman spectra of the PGO and Co-PGO samples. Co-PGO has three small peaks at 472, 514 and 679 cm^{-1}, which could be assigned to CoO E_g, F_{2g}, and A_{1g} bands, respectively. It further confirmed that the Co-PGO has Co(II) ions. Graphene has two distinguished peaks, i.e. D peak and G peak. The intensity ratio of the D peak to the G peak represents the defect properties of graphene

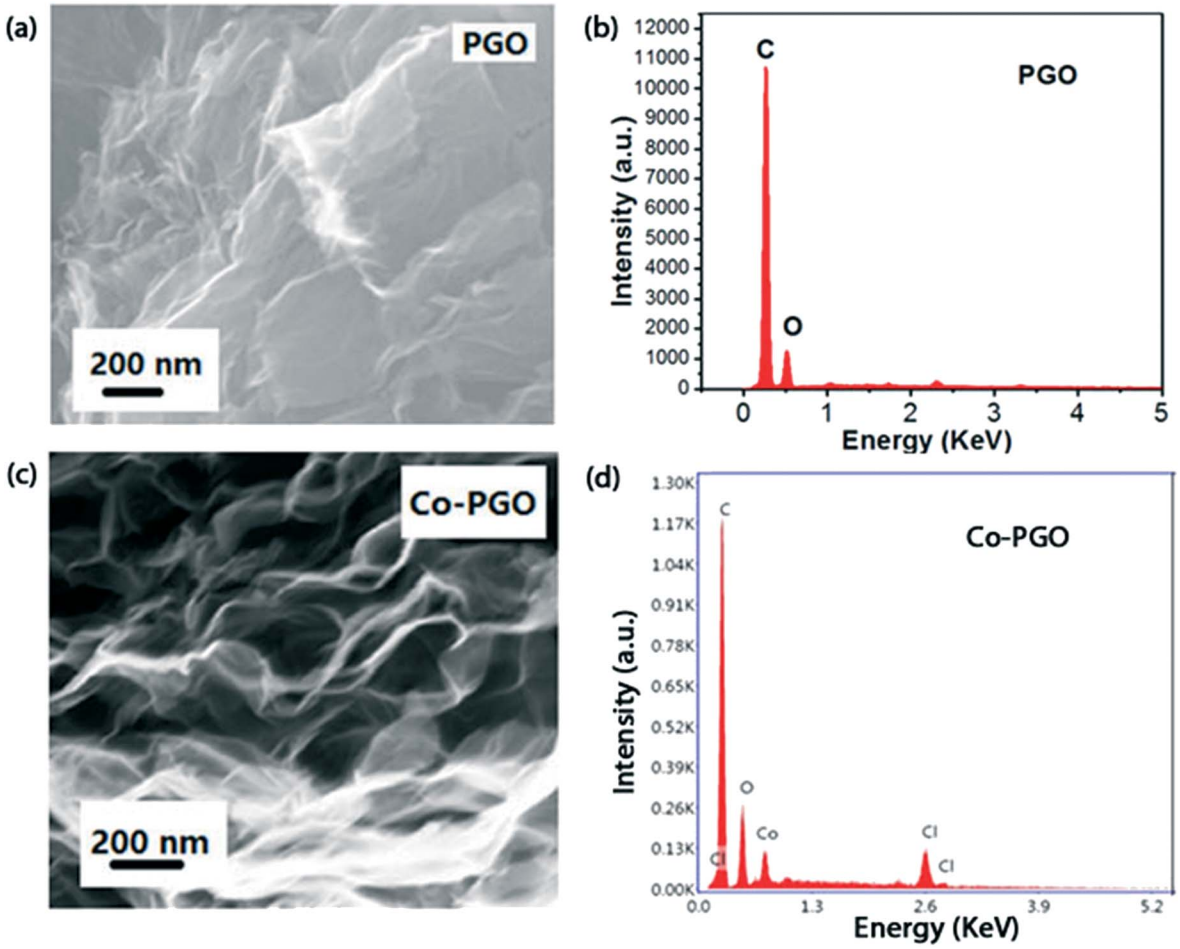

Fig. 1 SEM images of (a) PGO and (c) Co-PGO with their corresponding EDX spectra (b) and (d).

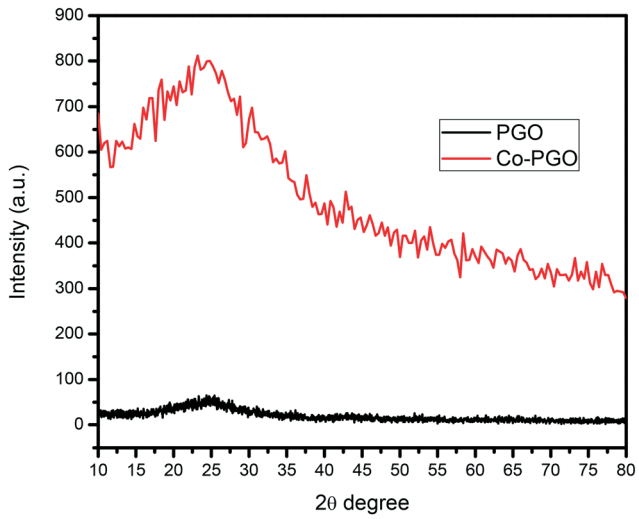

Fig. 2 XRD patterns of the PGO and Co-PGO samples.

surface. From the observation of the Raman spectra, the PGO and Co-PGO have a similar ratio of I_D/I_G, which means that the defect levels of these reduced GO samples are very similar.

Table 1 Gas adsorption data of the PGO and Co-PGO samples.

	PGO	Co-PGO
BET Surface Area (m^2/g)	154.2861	30.2373
BJH pore volume (cm^3/g)	0.04916	0.08747
Hydrogen adsorbed weight% at 293 K, 800 mmHg	0.031	0.084

Figure 4 shows the Co 2p XPS analysis of the Co-PGO sample. Even though the spectrum is relatively noisy due to the low concentration of cobalt, peaks at 781.4, 786.5, 797.28 and 803.4 eV are attributed to Co(II), in agreement with our assumption of the existence of ionic Co or atomic Co from XRD and Raman results (Figures 1 and 2, respectively). The source of Co(II) is from the precursor $CoCl_2$. The microwave process is short and the temperature is relatively low that the Co did not convert to a crystalline phase. Hence, from these results, Co still shows as ionic Co or atomic Co.

Figure 5 and Table 1 show the surface area data of the PGO and Co-PGO samples. It is clear that the Co-PGO has a relatively lower surface area than the PGO. It could be that Co(II) ions were intercalated into the GO layers, which contained residual moisture and functional groups like –OH groups, -COOH group, etc. This prevented the generation of water from the occupied functional groups, and decreased the amount of generated moisture vapor between GO layers. Therefore, vapor pressure

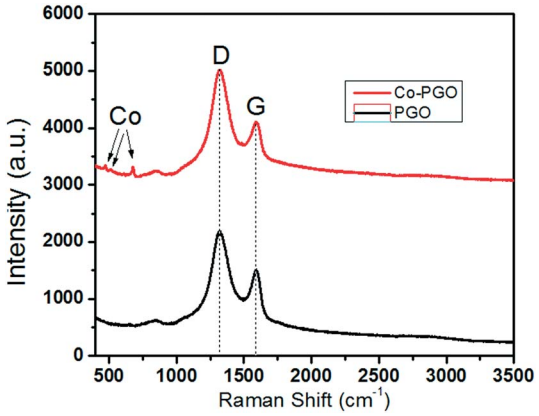

Fig. 3 Raman spectra of the PGO and Co-PGO samples.

generated in the Co-PGO was not as high as in the PGO, as a consequence, the Co-PGO showed lower surface area and pore volume than the PGO. Even though the Co-PGO has lower surface area, it still showed higher hydrogen storage capacity as discussed below because the Co(II) ions acted as a catalyst through the hydrogen spillover process.

Figure 6 presents the hydrogen isotherms of the PGO and Co-PGO. At 293 K and 800 mmHg, the Co-PGO can store 0.08wt% hydrogen, twice of the one observed for PGO. The developed surface area and the presence of Co(II) species on PGO present a promising materials for hydrogen adsorption. Based on the existent explanations of hydrogen storage mechanism, the Co(II) species might act as a spillover catalyst on the graphene surface. It helps to dissociate hydrogen molecules. It can also slightly react with H atoms and form unstable hydride, then H atoms transfer to the PGO surface and is stored between the PGO layers. Based on the best of our knowledge, this is the first study that Co(II) species are loaded on PGO and act as a hydrogen spillover catalyst.

As mentioned above, the Co-PGO also has great potential as an electrocatalyst for water splitting. It is an appealing method to generate hydrogen, since water is abundant and the by-product oxygen is safe and "green". However, at standard pressure and temperature, water

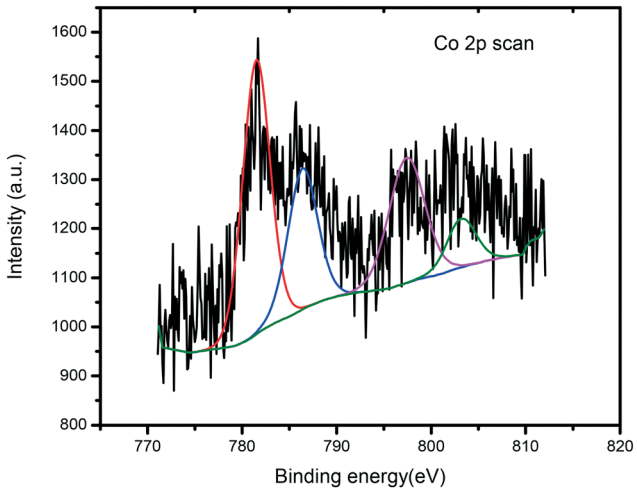

Fig. 4 Co 2p XPS analysis of the Co-PGO sample.

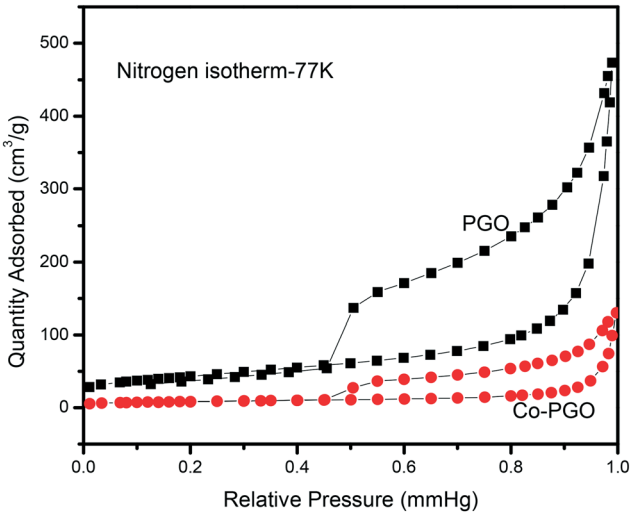

Fig. 5 BET surface area data of the PGO and Co-PGO samples.

splitting is not a thermodynamically favorable reaction.[27] To overcome this energy barrier, catalysts are usually used in the electrolysis of water. Pt is the most common used catalyst but it is not cost-effective.[28] Herein we explored the possibility to use the Co-PGO for catalytic HER.

Figure 7 presents the linear sweep voltammetry (LSV) of the PGO and Co-PGO. Compared to the PGO, the Co-PGO showed better catalytic HER activity with smaller overpotential and higher exchange current density. It is demonstrated that the Co-PGO has hydrogen storage capacity and hydrogen generation activity, and certainly a novel and attractive system with enormous potential for the hydrogen economy.

4. Conclusions

In this manuscript, we used a microwave popping method to synthesize popped Co(II)-PGO hybrid. Compared with popped PGO counterpart, Co-PGO demonstrated better hydrogen uptake capacity, lower HER overpotential and higher exchange current density. The Co(II) species loaded on the PGO can act not only as a hydrogen spillover catalyst

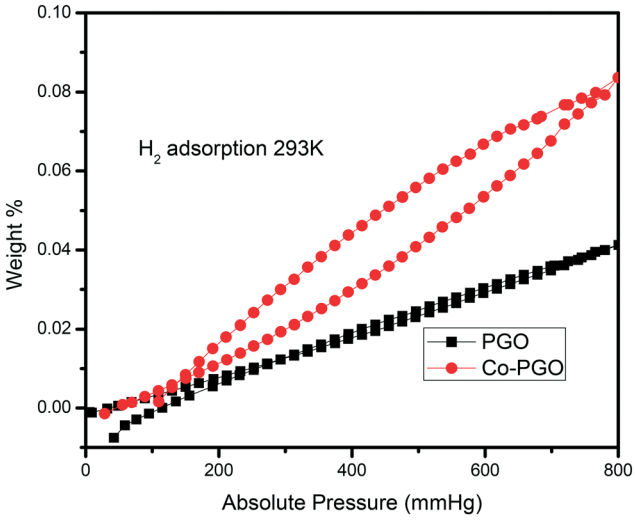

Fig. 6 Hydrogen isotherm of the PGO and Co-PGO samples.

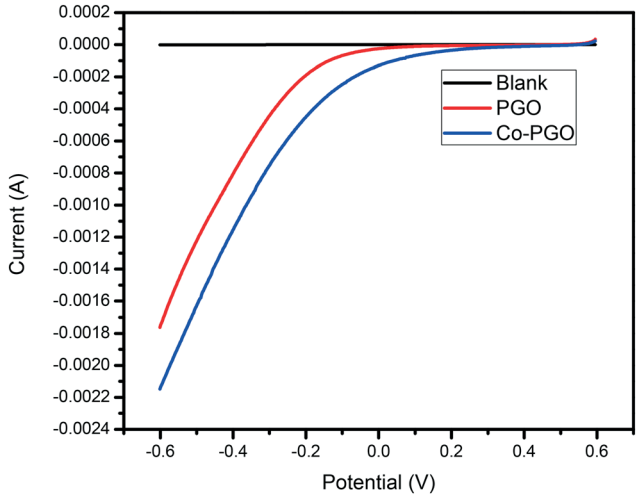

Fig. 7 LSV of the PGO and Co-PGO samples.

but also as a HER electrocatalyst. This paper is the first study to show that addition of Co(II) enhanced hydrogen storage for popped GO. With these results, the Co-PGO hybrid could be a promising material for hydrogen storage and hydrogen generation. It provides a novel system for future hydrogen energy processes, a combination of hydrogen generation and storage within the same material, a bifunctional catalyst.

Conflict of interest

There are no conflicts to declare.

Acknowledgements

The authors thank the financial support by the National Science Foundation under DMR (grant #1523577) and the USDA National Institute of Food and Agriculture (award #2015-38422-24059). The Department of Chemistry at the University of Texas Rio Grande Valley is grateful for the generous support provided by a Departmental Grant from the Robert A. Welch Foundation (Grant No. BX-0048).

References

1 Y. Mao, *Nanomater. Energy*, 2014, **3**, 103–128.
2 Q. Li, X. Sun, K. Lozano and Y. Mao, *J. Phys. Chem. C*, 2014, **118**, 13467–13475.
3 Q. Li, X. Sun, K. Lozano and Y. Mao, *Electrochim. Acta*, 2016, **222**, 232–245.
4 L. Wei and Y. Mao, *Int. J. Hydrogen Energy*, 2016, **41**, 11692–11699.
5 Y. Li and R. Yang, *J. Phys. Chem. C*, 2007, **111**, 11086–11094.
6 A. Lachawiec, G. Qi and R. Yang, *Langmuir*, 2005, **21**, 11418–11424.
7 A. Lueking and R. Yang, *Appl. Catal., A*, 2004, **265**, 259–268.
8 A. Lueking and R. Yang, *J. Catal.*, 2002, **206**, 165–168.
9 L. Wang and R. Yang, *J. Phys. Chem. C*, 2008, **112**, 12486–12494.
10 H. Nishihara, S. Ittisanronnachai, H. Itoi, L. Li, K. Suzuki, U. Nagashima, H. Ogawa, T. Kyotani and M. Ito, *J. Phys. Chem. C*, 2014, **118**, 9551–9559.
11 D. Owens, A. Han, L. Sun and Y. Mao, *Int. J. Hydrogen Energy*, 2015, **40**, 2736–2741.
12 R. Prins, *Chem. Rev.*, 2012, **112**, 2714–2738.
13 J. Li, J. Li, X. Zhou, Z. Xia, W. Gao, Y. Ma and Y. Qu, *ACS Appl. Mater. Interfaces*, 2016, **8**, 10826–10834.
14 C. McCrory, S. Jung, J. Peters and T. Jaramillo, *JACS*, 2013, **135**, 16977–16987.
15 J. Ahmed and Y. Mao, *J. Solid State Chem.*, 2016, **242**, 77–85.
16 J. Ahmed and Y. Mao, *Electrochim. Acta*, 2016, **212**, 686–693.
17 S. Mohan and Y. Mao, *ECS Trans.*, 2017, **77**, 1985–1994.
18 H. Fei, Y. Yang, Z. Peng, G. Ruan, Q. Zhong, L. Li, E. Samuel and J. Tour, *ACS Appl. Mater. Interfaces*, 2015, **7**, 8083–7.
19 J. Yu, G. Chen, J. Sunarso, Y. Zhu, R. Ran, Z. Zhu, W. Zhou and Z. Shao, *Adv. Sci.*, 2016, **3**, 1600060.
20 H. Jin, J. Wang, D. Su, Z. Wei, Z. Pang and Y. Wang, *JACS*, 2015, **137**, 2688–94.
21 Z. Wang, X. Hao, Z. Jiang, X. Sun, D. Xu, J. Wang, H. Zhong, F. Meng and X. Zhang, *JACS*, 2015, **137**, 15070–15073.
22 A. Dimiev and J. Tour, *ACS Nano*, 2014, **8**, 3060–3068.
23 J. Paredes, S. Villar-Rodil, A. Martinez-Alonso and J. Tascon, *Langmuir*, 2008, **24**, 10560–10564.
24 S. Dubin, S. Gilje, K. Wang, V. Tung, K. Cha, A. Hall, J. Farrar, R. Varshneya, Y. Yang and R. Kaner, *ACS Nano*, 2010, **4**, 3845–3852.
25 Y. Gao, X. Chen, J. Zhang, H. Asakura, T. Tanaka, T. Teramura, D. Ma and N. Yan, *Adv. Mater.*, 2015, **27**, 4688–4694.
26 Y. Zhu, S. Murali, M. Stoller, A. Velamakanni, R. Piner and R. Ruoff, *Carbon*, 2010, **48**, 2118–2122.
27 Y. Wen, Y. Xia and S. Zhang, *J. Power Sources*, 2016, **307**, 593–598.
28 Z. Zhang, W. Li, M. Yuen, T. Ng, Y. Tang, C. Lee, X. Chen and W. Zhang, *Nano Energy*, 2015, **18**, 196–204.